Interaction of the Staphylococcus aureus surface protein FnBPB with corneodesmosin involves two distinct, extremely strong bonds

Paiva, Telmo O; Viljoen, Albertus; da Costa, Thaina M; Geoghegan, Joan A; Dufrêne, Yves F

DOI:
10.1021/acsnanoscienceau.2c00036

Document Version
Publisher's PDF, also known as Version of record

Citation for published version (Harvard):
Paiva, TO, Viljoen, A, da Costa, TM, Geoghegan, JA & Dufrêne, YF 2023, 'Interaction of the *Staphylococcus aureus* surface protein FnBPB with corneodesmosin involves two distinct, extremely strong bonds', *ACS nanoscience Au*, vol. 3, no. 1, pp. 58-66. https://doi.org/10.1021/acsnanoscienceau.2c00036

ACS NANOSCIENCE Au
AN OPEN ACCESS JOURNAL OF THE AMERICAN CHEMICAL SOCIETY

pubs.acs.org/nanoau Article

Interaction of the *Staphylococcus aureus* Surface Protein FnBPB with Corneodesmosin Involves Two Distinct, Extremely Strong Bonds

Telmo O. Paiva,[‖] Albertus Viljoen,[‖] Thaina M. da Costa, Joan A. Geoghegan,* and Yves F. Dufrêne*

Cite This: https://doi.org/10.1021/acsnanoscienceau.2c00036 Read Online

ACCESS | Metrics & More | Article Recommendations | Supporting Information

ABSTRACT: Attachment of *Staphylococcus aureus* to human skin corneocyte cells plays a critical role in exacerbating the severity of atopic dermatitis (AD). Pathogen-skin adhesion is mediated by bacterial cell-surface proteins called adhesins, including fibronectin-binding protein B (FnBPB). FnBPB binds to corneodesmosin (CDSN), a glycoprotein exposed on AD patient corneocytes. Using single-molecule experiments, we demonstrate that CDSN binding by FnBPB relies on a sophisticated two-site mechanism. Both sites form extremely strong bonds with binding forces of ∼1 and ∼2.5 nN albeit with faster dissociation rates than those reported for homologues of the adhesin. This previously unidentified two-binding site interaction in FnBPB illustrates its remarkable variety of adhesive functions and is of biological significance as the high strength and short bond lifetime will favor efficient skin colonization by the pathogen.

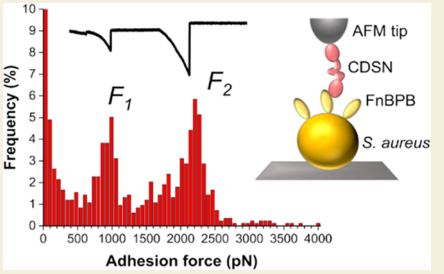

KEYWORDS: *Staphylococcus aureus, FnBPB, corneodesmosin, extremely strong bonds, two-binding site mechanism*

INTRODUCTION

Infectious diseases caused by bacterial pathogens are one of the most concerning threats to public health.[1] Among these, *Staphylococcus aureus* causes various diseases in humans, including cardiovascular and respiratory infections, surgical wound and indwelling medical device-related infections, and serious skin disorders and diseases.[2,3] About 20% of healthy humans are persistently colonized by *S. aureus*, which increases their risk of serious infection.[4] Individuals affected by the chronic inflammatory skin disease atopic dermatitis (AD) are particularly susceptible to skin colonization by *S. aureus*,[3,5] which exacerbates AD symptoms and the severity of the disease.[6,7] A better understanding of the specific molecular mechanisms by which the pathogen binds to human skin would greatly benefit endeavors to develop efficient treatments for bacterial colonization of AD skin.

Adhesion of *S. aureus* to corneocytes from the stratum corneum, which represents the outermost layer of the epidermis,[8−10] is mediated by various bacterial cell wall-anchored proteins (adhesins), including fibronectin-binding protein B (FnBPB) and clumping factor B (ClfB),[8−11] which bind to specific ligands like loricrin, keratin, and fibrinogen (Fg). On AD corneocytes, both FnBPB and ClfB interact with the N-terminal region of the corneocyte glycoprotein corneodesmosin (CDSN).[11] While CDSN is not abundant on the surface of corneocytes from healthy individuals,[12] it becomes surface-exposed in AD patients where it decorates the tips of "villus-like" projections when levels of the skin's natural moisturizing factors are low.[10,13]

The amino acid sequence of CDSN is dominated by serine and glycine residues. These residues are mainly organized into domains at the protein's N- and C-termini, where they appear as tandem repeats that are predicted to fold into two highly flexible secondary structures called serine-glycine-rich loops.[14] The serine-glycine-rich loops display adhesive properties[12] and are involved in CDSN-CDSN homophilic interactions.[15] FnBPB and ClfB bind to the N-terminal region of CDSN where the first serine-glycine-rich loop is located.[11]

FnBPB comprises a secretory signal sequence at the N-terminus, an N-terminal A region, a large central domain composed of multiple tandemly arranged fibronectin (Fn)-binding repeats, and a C-terminal cell wall-anchoring motif (Figure 1A).[16] The A region, where Fg and elastin binding sites are located, is predicted to fold into three separate domains N1, N2, and N3. N2 and N3 form IgG-like folds that bind multiple ligands through the multistep dock, lock, and latch (DLL) mechanism.[17−19] In the past years, DLL complexes have been shown to have extremely high mechanical stability, being able to sustain forces that are much larger than the vast majority of the receptor−ligand interactions studied so far.[20−24] FnBPB binds to Fg and elastin using the DLL interaction but uses another mechanism to bind plasminogen.[25−28]

Despite the medical importance of the FnBPB−CDSN interaction in AD, its molecular details are currently unknown.

Received: July 19, 2022
Revised: September 30, 2022
Accepted: September 30, 2022

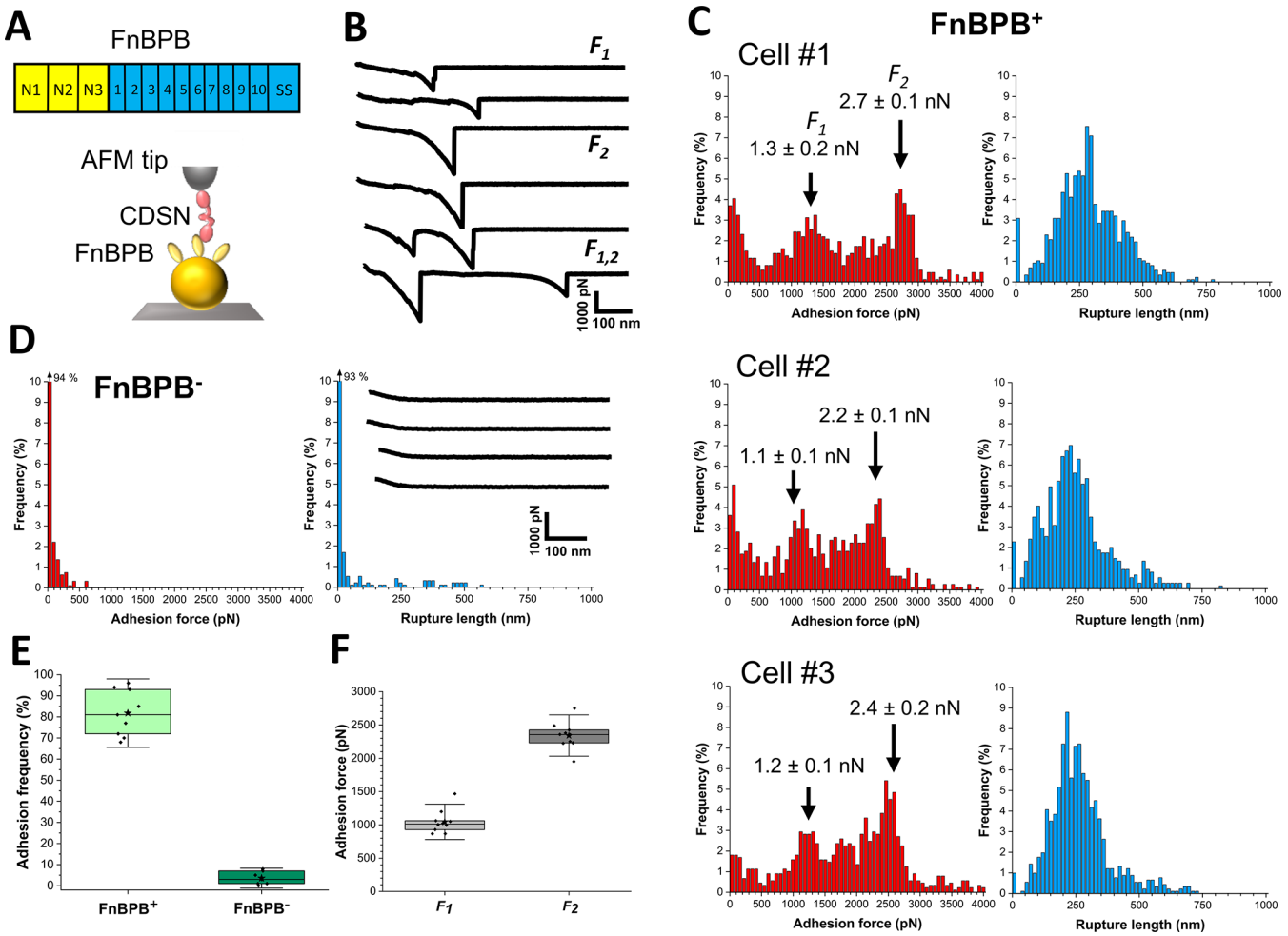

Figure 1. Interaction between the *S. aureus* FnBPB and human corneodesmosin involves two extremely strong bonds. (A) Scheme of FnBPB modular architecture and the single-molecule force spectroscopy (SMFS) experimental setup used to study the FnBPB−CDSN interaction forces. (B) Representative retraction profiles recorded when probing *S. aureus* cells expressing FnBPB (FnBPB$^+$) with an AFM tip modified with CDSN as depicted in (A). (C) Adhesion force (left) and rupture length (right) histograms of three different FnBPB$^+$ cells probed with AFM tips modified with CDSN (contact time: 50 ms; approach and retraction speeds: 1000 nm s^{-1}; total number of curves for each cell n = 1024; for more cells, see Figure S1A). Arrows point to adhesion force maxima defining two distinct high-adhesion-force-regime populations. (D) Adhesion force and rupture length data for a representative FnBPB$^-$ cell (for more cells, see Figure S1B). The inset on the right shows four representative retraction profiles. (E) Box plot of the adhesion frequency of FnBPB$^+$ and FnBPB$^-$ *S. aureus* strains (n = 9 and 7 cells, respectively). (F) Box plot showing the adhesion force values that characterize the two distinct populations (F_1 and F_2) for 10 different FnBPB$^+$ *S. aureus* cells. Stars indicate mean values, lines indicate medians, boxes indicate 25−75% quartiles, and whiskers indicate standard deviation (SD).

Consequently, there is an urgent need for new molecular data on CDSN binding by FnBPB, which could help contribute to innovative strategies to prevent or treat *S. aureus* skin colonization in AD. Here, we investigate the molecular basis of this interaction using single-molecule experiments.[29−32] The results show that the FnBPB−CDSN interaction is extremely strong and features two distinct populations of binding forces at 1 and 2.5 nN. These binding forces do not show a catch bond behavior where bond strength is dramatically enhanced by tensile loading, as in known DLL interactions. Dissociation rates are much faster than for highly stabilized DLL complexes and neither of the bonds is inhibited by a peptide mimicking the C-terminal segment of the Fg γ-chain. Our findings show that FnBPB binds to CDSN through a novel mechanism involving two distinct ligand-binding sites, and favor a model in which the two sites are allosterically linked.[33,34]

RESULTS

FnBPB−CDSN Interaction Involves Two Populations of Extremely Strong Binding Forces

We used single-molecule force spectroscopy (SMFS; Figure 1A) with human CDSN-functionalized tips to probe living *S. aureus* cells expressing FnBPB (FnBPB$^+$). Figure 1B,C presents representative force curves and the distributions of adhesion forces and rupture lengths for three independent FnBPB$^+$ cells (for more cells, see Figure S1A). In 80% of the curves (from a total of 5120 curves from 5 cells), we observed adhesive events, with a wide distribution of forces, up to ∼3 nN. Out of the population of adhesive curves, 75% featured single well-defined force peaks, while 25% of the curves showed two consecutive, well-defined force peaks (Figure 1B). These binding events were specific to FnBPB, as adhesion was abrogated in *S. aureus* cells lacking FnBPB (FnBPB$^-$) (Figure 1D,E; for more cells, see Figure S1B), the binding frequency dropping from 80 to 4% (from a total of 7189 curves from 7 cells).

https://doi.org/10.1021/acsnanoscienceau.2c00036
ACS Nanosci. Au XXXX, XXX, XXX−XXX

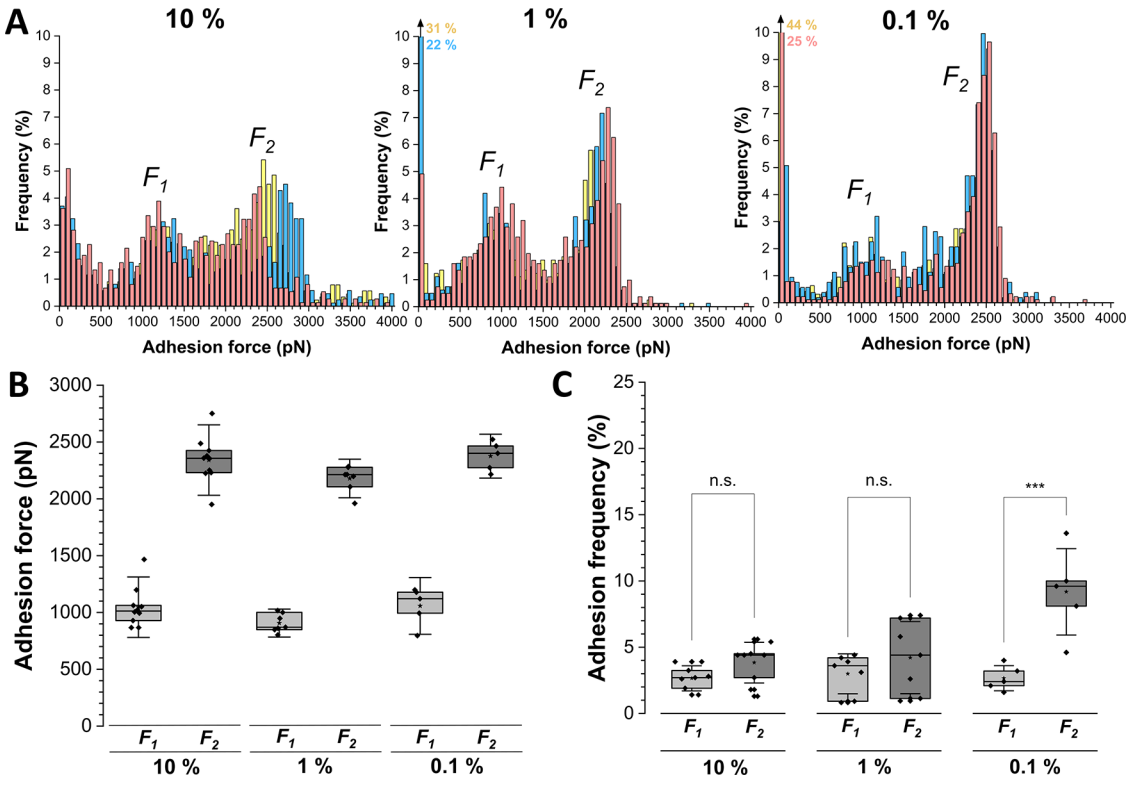

Figure 2. Lowering the CDSN concentration on the AFM tip does not alter the bimodal force distribution. (A) Adhesion force histograms obtained for three FnBPB$^+$ cells (3 different colors) probed with AFM tips modified with varying levels of CDSN. The concentration of CDSN on the tips was lowered by decreasing the amount of 16-mercaptododecahexanoic acid. (B) Box plots of the force values and (C) adhesion frequencies for the two distinct force populations obtained with AFM tips exposing varying densities of CDSN. At least five different cells were probed with each CDSN tip. ***p-value $\leq$ 0.001, determined by a two-sample t-test in Origin.

Close examination of the adhesion histograms revealed two maxima (Figure 1F), one centered at 1.0 ± 0.1 nN (hereafter referred to as "F_1"; data pooled from n = 636 adhesive curves on 5 cells), the other at 2.3 ± 0.2 nN ("F_2"; n = 826 adhesive curves on 5 cells). We note that a small fraction of adhesive events (20% from all cells) were much weaker (166 ± 42 pN), most likely resulting from a combination of nonspecific interactions, which are expected given the diversity of constituents present at the cell surface, and FnBPB−CDSN interactions occurring outside of the ligand-binding responsible for highly stable binding. Force curves were similar when analyzing multiple cells from independent cultures and using different ligand-coated tips. They did not change when recording consecutive force curves (1024) on the same cell, implying that the measurements did not alter the conformational and functional properties of the cell surface adhesins and of the ligands. Altogether, these observations show that rupture of the FnBPB−CDSN complex always involves two distinct populations of extremely strong binding forces.

We then asked whether the F_1 and F_2 forces result from the rupture of single bonds. Similar adhesion force distributions with only two maxima always centered at ∼1 and ∼2.5 nN were reproducibly observed from one tip or one cell to another, including those from independent preparations. When multiple bond-breaking events simultaneously occur at a high frequency, a broad multimodal distribution reflecting multiples of the weakest unit force should be observed. Clearly, this was not the case since no maxima were observed at either 3 or 4 nN (Figure 1C).

To provide a direct, unambiguous demonstration that FnBPB and CDSN were engaged in two single and distinct bonds, we decreased the surface density of the ligand on the tip (Figure 2), using gold-coated tips bearing 1 or 0.1% COOH groups, instead of 10% as used above. Strikingly, force distributions centered at ∼1 and ∼2.5 nN (Figure 2A,B) were similar to those at 10% density, except that as the ligand concentration decreased, the two force distributions became narrower (Figure 2A). If multiple bonds were to be probed in our standard conditions (10%), we should observe that dilution of the ligand density leads to a shift toward lower forces corresponding to the unit force of single bonds, which was not the case. Narrowing of the two force distributions is likely to result from the lower number of ligands on the tip and hence the potential binding geometries. Finally, we note that while the probability of observing F_1 forces remained unchanged, the probability of observing F_2 forces (Figure 2C) substantially increased, from 3.8 and 4.1% at 10 and 1% ligand density, to 10.3 at 0.1% density (means from 5 cells in each condition; n = 3883 (10%), 2921 (1%) and 2682 (0.1%) adhesive curves, respectively). This unusual behavior indicates that they do not result from the simultaneous rupture of two identical 1 nN bonds but that they rather reflect two single bonds of different molecular nature, associated with two distinct binding sites.

Most adhesive interaction forces ruptured at ∼250 nm (Figure 1C, right panels; 237 ± 50 nm, n = 8166 adhesive curves from 10 cells). Assuming that each amino acid contributes 0.36 nm to the contour length of a polypeptide chain, the length of a fully extended FnBPB protein (957

https://doi.org/10.1021/acsnanoscienceau.2c00036
ACS Nanosci. Au XXXX, XXX, XXX−XXX

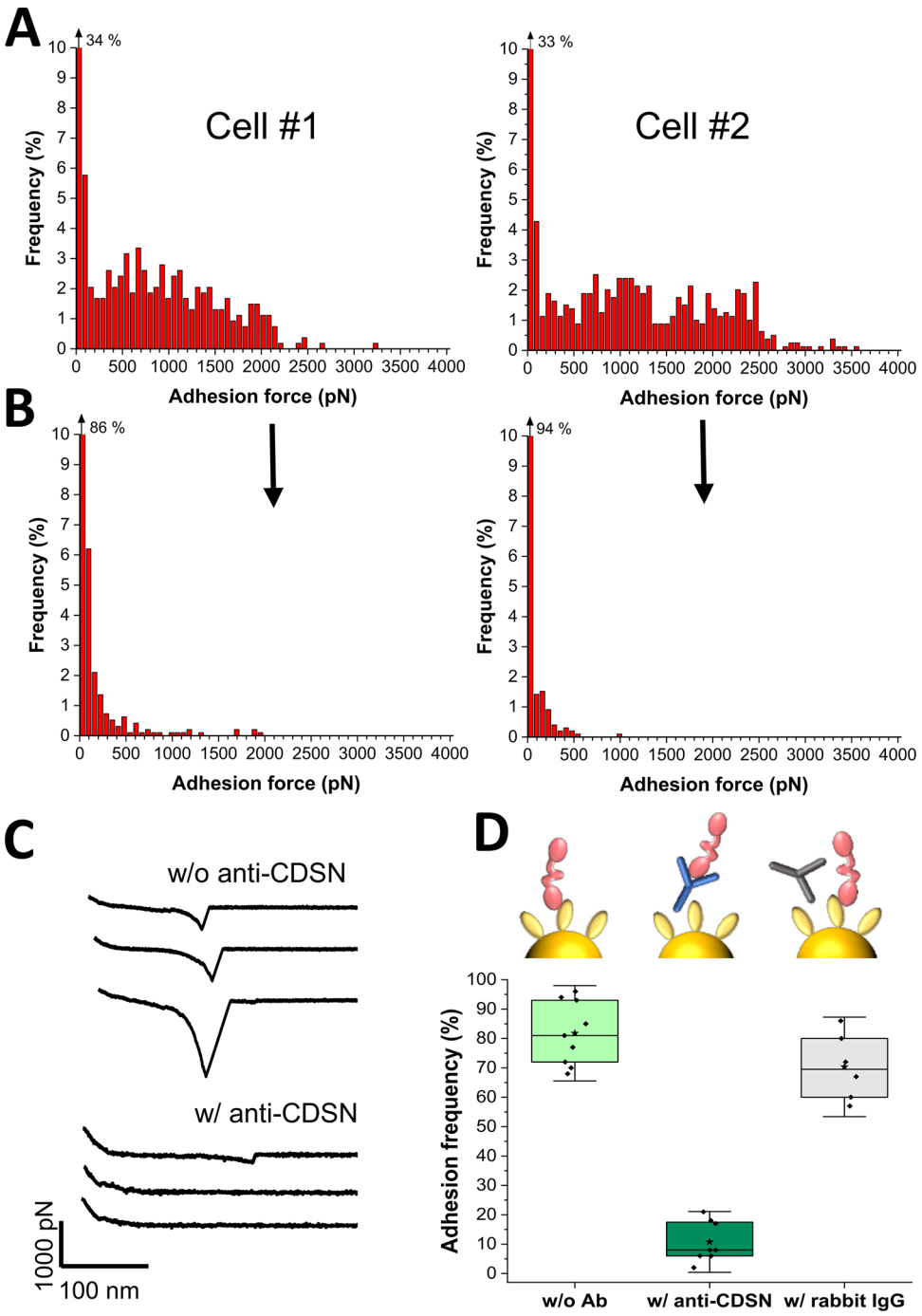

Figure 3. Incubation with an anti-CDSN antibody specifically inhibits the FnBPB−CDSN interaction. (A) Adhesion force histograms of two representative FnBPB$^+$ cells probed with an AFM tip modified with CDSN. (B) Data obtained for the same cells as in (A) after treatment of the same AFM tip with an antibody targeting the N-terminus of CDSN (for more cells, see Figure S2). (C) Representative retraction profiles recorded when probing FnBPB$^+$ cells with CDSN-modified tip before and after treatment with an anti-CDSN antibody. (D) Box plots of the adhesion frequency of FnBPB$^+$ cells before and after tip treatment with an anti-CDSN antibody (9 cells; 1024 curves for each cell). In addition, six FnBPB$^+$ cells were probed with an AFM tip treated with rabbit IgG as a negative control (Figure S3). Stars indicate mean values, lines indicate medians, boxes indicate 25−75% quartiles, and whiskers indicate SD.

amino acids) is expected to be 340 nm, thus higher than what we observe. This indicates that applying forces as high as 2.5 nN does not lead to the full unfolding of the adhesin. It is more likely that the Fn-binding repeats would fully unfold as they are intrinsically disordered.[19] By contrast, we expect the tertiary structure of the N domains, specifically N2N3, to be required to support a high mechanostability of the bonds, meaning they are probably not fully unfolded. In addition, we must also consider that stretching of the CDSN ligand may to some extent contribute to the observed extensions.

Strong Binding Involves the CDSN N-Terminus and Probably Does Not Involve a Canonical DLL Interaction

FnBPB binds to the CDSN glycine-serine-rich loop, a secondary structure located at the N-terminus of the protein.[11,12] To test whether the ∼1 nN and/or the ∼2.5

https://doi.org/10.1021/acsnanoscienceau.2c00036
ACS Nanosci. Au XXXX, XXX, XXX−XXX

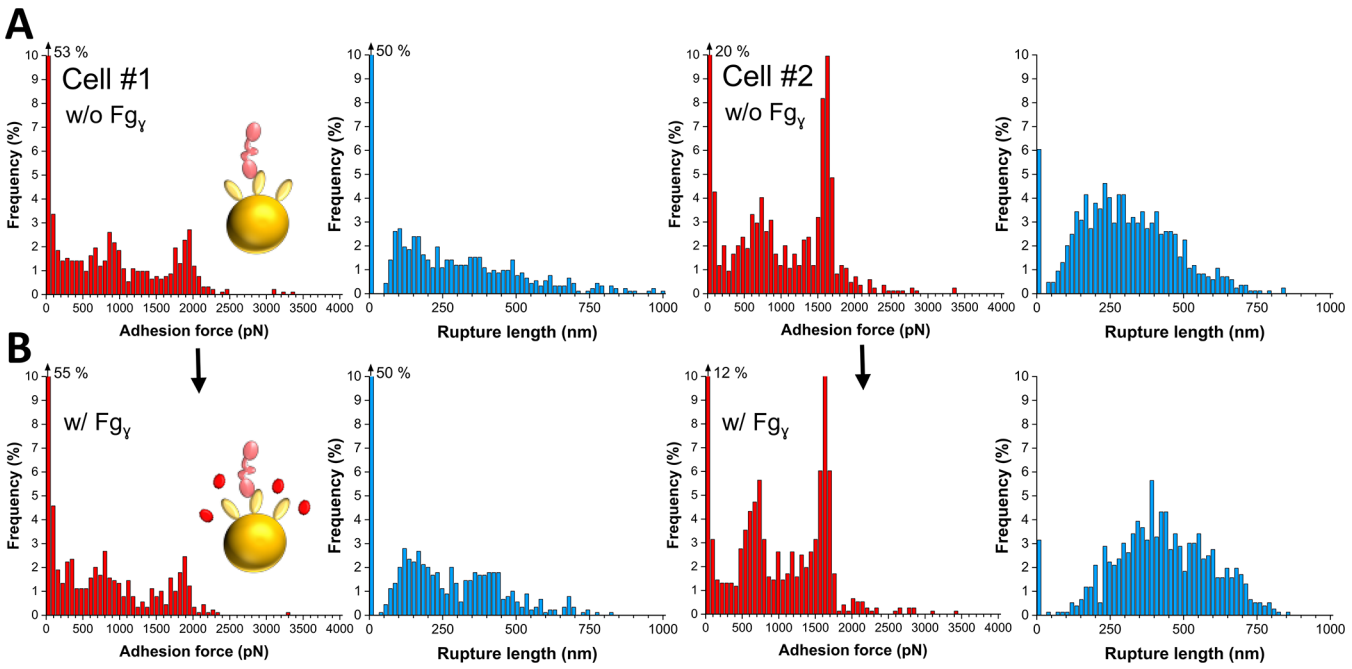

Figure 4. FnBPB−CDSN interaction is not altered by the fibrinogen γ-chain peptide. (A, B) Adhesion force and rupture length histograms of two representative FnBPB$^+$ cells (total of n = 1024 curves for each cell) probed with an AFM tip modified with CDSN before (A) and after (B) addition of 0.1 mg mL^{-1} Fg$_\gamma$.

nN forces exclusively involve this region, inhibition assays were performed using an IgG directed against the CDSN N-terminus. When CDSN-tips were treated with this IgG, adhesion forces were abrogated as can be seen for cells probed with independent tips in Figures 3 and S2. Analysis of more cells revealed that the adhesion probability dropped from 80 to 11% (9 cells, 6 tips, 9216 curves), and that strong F_1 and F_2 forces were never observed. By contrast, the forces were not altered when using a control nonspecific IgG (Figures 3D and S3). These results show that both the high and ultrahigh adhesion forces originate from the binding of FnBPB to the CDSN N-terminus.

We next wondered whether the strong binding forces may result from a DLL mechanism as the N2N3 domains of FnBPB have been shown to support CDSN binding.[11] Fg binding by several adhesins (FnBPA, FnBPB, and ClfA) occurs through the DLL mechanism, which results from the interaction between N2N3 subdomains and the extreme C terminus of the γ-chain of Fg.[35−37] We therefore carried out inhibition assays in which we added a 17-mer γ-chain C-terminal peptide (GEGQQHHLGGAKQAGDV), corresponding to an FnBPB binding site in Fg, to test whether it blocks the strong adhesive forces. In Figure 4, it can be seen that the peptide had virtually no effect on the force data, thus showing that the affinity of FnBPB for the γ-chain peptide is far weaker than the affinity for CDSN. This finding strongly suggests that strong binding forces do not originate from a canonical DLL mechanism, which is further supported by the dynamics of the unbinding process.

Dynamic Force Spectroscopy Supports a Non-DLL, Two-Binding Site Mechanism

We explored the dynamics of the FnBPB−CDSN interaction by measuring the adhesion forces (F) while varying the loading rate (LR), i.e., the rate at which force is applied (Figure 5; estimated from the force *vs* time curves). The resulting dynamic force spectroscopy (DFS) plot (data pooled from 10,374 adhesive curves on 4 FnBPB$^+$ cells), Figure 5A, featured a diffuse distribution with several clouds resulting from the different pulling speeds. Discrete ranges of LRs were binned and the force distributions were plotted as histograms (Figure 5B). As expected for classical specific receptor−ligand bonds, the forces within F_1 and F_2 populations shifted progressively toward higher values when increasing the LR.[38] This contrasts with the dramatic switch in force usually observed for DLL interactions,[39,40] that result from a catch bond behavior.[41] From the histograms, we extracted the most probable adhesion force for F_1 and F_2 forces. As predicted by the Bell−Evans (BE) theory, both binding forces (F) increased linearly with the logarithm of the LR.[29] Fitting with the BE model yielded a position of the energy barrier that separates the bound from the unbound state of x_u = 0.02 nm for both F_1 and F_2, and off-rate constants at thermal equilibrium of k^0_{off} = 1.2 ± 0.8 s^{-1} and k^0_{off} = 0.003 ± 0.006 s^{-1} for F_1 and F_2, respectively. These values are orders of magnitude higher than that of DLL complexes, in the range of 10^{-9}−10^{-13} s^{-1},[20,22,24,41] meaning that the FnBPB−CDSN bond lifetime is much smaller than canonical DLL bonds.

We also studied the influence of the interaction time on the magnitude and distribution of the forces, while keeping the pulling speed constant. Force curves recorded using an interaction time of 300 ms (Figure S4B) instead of 50 ms (Figure S4A) showed that the duration of contact had absolutely no effect on the probability and strength of adhesion. This confirms once again that F_2 forces are not generated by the rupture of multiple F_1 bonds in parallel and, moreover, that bond formation is fast. This lack of time dependency is in contrast to the prototypical SdrG−Fg DLL complex,[20] where the adhesion probability increases with the duration of contact between the interacting molecules, an effect suggesting that the conformational changes needed for binding require a sufficient amount of time. Together with our

https://doi.org/10.1021/acsnanoscienceau.2c00036
ACS Nanosci. Au XXXX, XXX, XXX−XXX

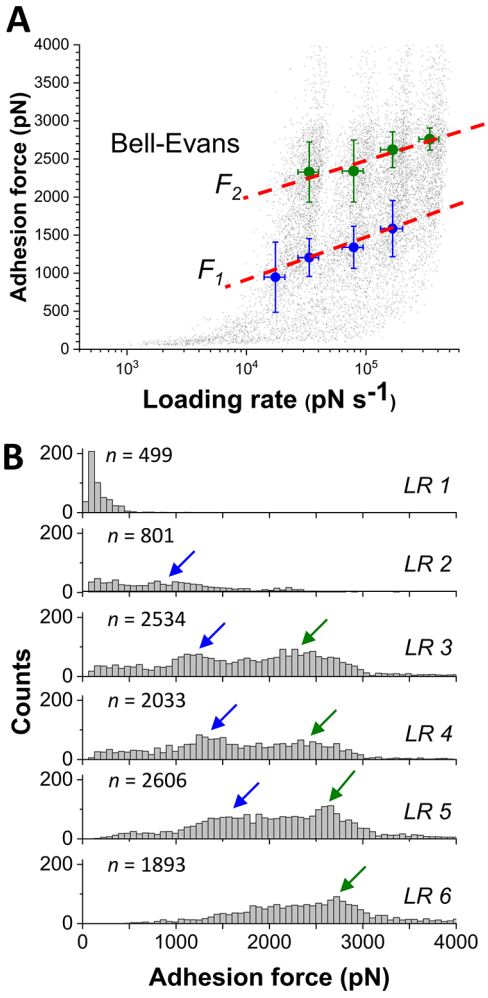

Figure 5. Dynamics of the FnBPB−CDSN interaction. (A) DFS plot showing the adhesion force as a function of the logarithm of the loading rate (LR) applied during retraction while keeping constant the interaction time (50 ms) and the approach speed (1000 nm s^{-1}). Data pooled from four FnBPB$^+$ cells (total of n = 10,374 adhesive events). Bell−Evans fits (dashed red line) through the most probable F_1 and F_2 forces showing the expected loading-rate dependency and x_u = 0.02 nm and k_{off}^0 = 1.2 ± 0.8 s^{-1} for F_1 and x_u = 0.02 nm and k_{off}^0 = 0.003 ± 0.006 s^{-1} for F_2. Error bars represent the standard deviations. (*B*) Adhesion force histograms as a function of discrete ranges of loading rates: LR1 < 10,000 pN s^{-1}, 10,000 < LR2 < 22,000 pN s^{-1}, 22,000 < LR3 < 49,000 pN s^{-1}, 49,000 < LR4 < 106,000 pN s^{-1}, 106,000 < LR5 < 230,000 pN s^{-1}, 230,000 < LR6 < 400,00 pN s^{-1}. Note that only force values > 500 pN were considered to calculate the most probable F_1 and F_2 averaged data points shown in (A), excluding force values belonging to LR1 from panel (B). The arrows in panel (B) indicate the maximum force values extracted from the force distributions equivalent to the most probable F_1 and F_2 data points shown in panel (A).

fast dissociation rate, these observations show that, unlike other DLL systems, bond formation and dissociation are fast processes.

DISCUSSION

Binding of FnBPB to CDSN promotes the attachment of *S. aureus* to the skin of AD patients via molecular interactions that are currently unknown. Here we have shown that FnBPB binds CDSN through an unusual, previously undescribed two-site mechanism. Our main findings are as follows: (i) the FnBPB−CDSN interaction features a bimodal force distribution, with binding strengths of ∼1 and ∼2.5 nN; (ii) inhibition assays with antibodies demonstrate these forces result from binding to the N-terminal region of the ligand; (iii) the Fg γ-chain peptide has no effect on the probability and strength of adhesion, suggesting that the Fg γ-chain does not compete with the CDSN binding site within FnBPB; (iv) unlike the well-characterized DLL catch bonds, FnBPB−CDSN forces are not dramatically enhanced by tensile loading, but rather increase gradually along each force population; and (v) the bond dissociation rates are orders of magnitudes faster than for highly stabilized DLL complexes, and the binding probability is not time-dependent. Collectively, our results demonstrate that during colonization of AD skins, FnBPB engages in a two-binding site interaction that differs from that of previously described DLL-like mechanisms, thus emphasizing the multifunctional adhesion mechanisms of this adhesin. Nevertheless, we do not exclude the possibility that a variation of DLL may be implicated in our proposed two-site binding mechanism. Indeed, variations of the prototypical SdrG DLL mechanisms have been reported.[36,42,43]

The very high forces of the FnBPB−CDSN bonds are similar to those of covalent bonds at comparable loading rates,[44] and an order of magnitude stronger than the vast majority of receptor−ligand bonds studied so far, including specific cell adhesion bonds that typically sustain forces in the 50−150 pN range.[29,45−48] The streptavidin−biotin pair had long been considered as forming the strongest receptor−ligand bond with a force of 100−250 pN, as measured by AFM and other force-measuring techniques. In the past years, however, several bacterial molecular complexes have been found to feature much higher binding forces,[23,39,49] including the cohesin−dockerin complexes of cellulolytic bacteria[49−51] and the staphylococcal adhesins SdrG, ClfA, and ClfB that engage in DLL interactions with forces in the 1.5−2 nN range.[21−24] It is remarkable that FnBPB can bind CDSN with even higher forces, yet through a different mechanism.

An interesting observation is that the FnBPB−CDSN interaction involves extremely strong forces despite a moderate biochemical affinity, in the μM range.[11] An explanation for this is that the unbinding pathway of FnBPB under force differs from that at equilibrium, in the absence of force, a phenomenon described for bacterial multicomponent protein networks called "cellulosomes".[52] This suggests that non-equilibrium single-molecule force experiments are more relevant than classical equilibrium bioassays when it comes to understanding the binding mechanisms of bacteria that have to withstand the physical stresses during colonization of the skin (cell surface contacts, scraping, or epithelial turnover).[53]

It is intriguing that the CDSN−FnBPB interaction outperforms canonical DLL interactions (1.5−2 nN) in terms of binding strength. A possible explanation for our results is that binding geometry plays a role[54] where CDSN binds at different angles to the binding sites located in FnBPB. Another explanation is a model in which two binding sites in FnBPB are allosterically linked, binding at one site may have a positive allosteric influence on the binding strength of the other site.[33,34] Our data and proposed mechanism are reminiscent of the behavior of the mammalian cell serotonin receptor,[34] for which AFM unraveled two populations of binding forces in an allosterically modulated interaction with the ligand S-citalopram. Like here, force curves for the S-citalopram interaction with the serotonin receptor mainly exhibited

https://doi.org/10.1021/acsnanoscienceau.2c00036
ACS Nanosci. Au XXXX, XXX, XXX−XXX

distinct single unbinding events at two discrete force values. To the best of our knowledge, this is the first time that such an allosteric two-site mechanism is proposed for a staphylococcal adhesin.

A well-known example of an allosterically regulated adhesin is the *Escherichia coli* FimH protein that forms catch bonds with mannose ligands. Force-induced structural alterations in one part of the protein are linked to a shift from a low- to a high-affinity conformation of the ligand-binding site located in another part of the molecule.[55] Our results do not favor a catch bond mechanism, usually associated with DLL complexes,[41] supporting the notion that the FnBPB−CDSN interaction involves a new type of mechanism, possibly employing features of DLL, but involving two allosterically linked binding sites. Further studies using *S. aureus* mutant strains expressing different forms of FnBPB, e.g., lacking the CDSN-binding region, will help to decipher the involvement of the two binding sites and, moreover, the hypothesized allosteric relation between them. Furthermore, solving the crystal structure of FnBPB in complex with CDSN combined with simulation studies is needed to provide atom-level details of the binding mechanism.

We speculate that the short-lived and extremely strong forces identified here may play an important role in efficient skin colonization in that short duration of the bonds may favor the detachment of the pathogens, and therefore the colonization of new skin sites. The two-site interaction mechanism is a promising target for the design of innovative antiadhesion therapeutics to prevent and treat AD infections.

METHODS

Bacterial Strains and Growth Conditions

We used *S. aureus* SH1000 4X carrying the empty pALC2073 plasmid background control strain (FnBPB$^-$) and *S. aureus* SH1000 4X (pALC2073:*fnbB*) expressing FnBPB (FnBPB$^+$).[11,56] Bacteria were cultured in TSA plates containing 10 μg mL^{-1} chloramphenicol overnight, at 37 °C. A single colony was transferred to 10 mL of TSB containing 10 μg mL^{-1} chloramphenicol and cultured overnight, at 37 °C, under shaking. Stationary phase cultures were then harvested three times by 5 min centrifugation steps at 2000*g*, washed with TSB, diluted to an OD_{600} = 0.05 in the same culture medium containing 10 μg mL^{-1} chloramphenicol, and cultured under shaking at 37 °C. When an OD_{600} = 0.17 was reached, 300 ng mL^{-1} anhydrotetracycline was added to the cultures, which were allowed to further grow until OD_{600} = 0.35 (early exponential phase).

Sample Preparation

Bacterial cells were pelleted by centrifugation, washed in PBS, and resuspended in the same buffer. A volume of 200 μL of 100 times diluted cellular suspension was subsequently deposited on a polystyrene Petri dish, and the cells were allowed to adhere for at least 20 min. Finally, three rinsing steps with PBS were performed and the Petri dish filled with 2 mL of this buffer prior to the AFM experiments.

Functionalization of AFM Tips

Gold cantilevers (PNP-Tr-Au, Nanoworld) were thoroughly rinsed with water and ethanol, dried with N_2 flow, and further cleaned in a UV-ozone chamber for 10 min. They were then immersed overnight in a 1 mM solution containing a mixture of 16-mercaptododecahexanoic acid (10%; Sigma-Aldrich) and 1-mercapto-1-undecanol (90%; Sigma-Aldrich) in ethanol and protected from light. For some experiments, 16-mercaptododecahexanoic acid was used at 1 or 0.1%. Then, cantilevers were rinsed with ethanol, dried with N_2, and immersed in an aqueous solution containing 10 mg mL^{-1} *N*-hydroxysuccinimide (NHS) and 25 mg mL^{-1} 1-ethyl-3-(3-dimethylaminopropyl)-carbodiimide (EDC) for 30 min. After rinsing with ultrapure water, the cantilevers were immersed in a 0.1 mg mL^{-1} corneodesmosin (CDSN, LSBio) solution in PBS for 1 hour and finally rinsed with PBS.

AFM Force Spectroscopy

Single-molecule force spectroscopy (SMFS)[32] was performed at room temperature (20 °C), using a JPK NanoWizard 4 NanoScience AFM. CDSN cantilevers were calibrated by the thermal noise method, yielding spring constants ranging from 0.03 to 0.07 N.m^{-1}. Force−distance curves were recorded on 500 nm × 500 nm areas on the top of single bacterial cells, employing the force mapping mode with the following parameters: 32 × 32 force curves, constant approach and retraction speeds of 1 μm s^{-1}, ramp length of 1 μm, applied force of 250 pN, and additional dwell time of 0 or 250 ms, corresponding to an actual time of contact of ∼50 and 300 ms. For dynamic force spectroscopy, the retraction speed was varied from 1 to 2.5, 5, and 10 μm s^{-1}. All force data were analyzed with the JPK Data Processing software, and statistical analysis was carried out using the Origin software (OriginPro 2021).

Inhibition AFM Assays

We tested the influence of a polyclonal antibody directed against the CDSN N-terminus (LSBio). After having recorded a force map on top of a single bacterium, the CDSN tip was exposed to a 10 μg mL^{-1} anti-CDSN solution in PBS for 1 h and a new force map was then recorded on the same cell. A rabbit IgG antibody (LSBio) was used as a control (10 μg mL^{-1}). We also tested the influence of the 17-mer fibrinogen γ-chain C-terminal peptide (GEGQQHHLGGAK-QAGDV; GenScript). Force maps were recorded sequentially on the top of the same cell, before and after peptide injection at a final concentration of 0.1 mg mL^{-1}. All force maps were registered 15 min after peptide injection.

ASSOCIATED CONTENT

Supporting Information

The Supporting Information is available free of charge at https://pubs.acs.org/doi/10.1021/acsnanoscienceau.2c00036.

Additional FnBPB$^+$ and FnBPB$^-$ cells probed by single-molecule force spectroscopy (Supporting Figure 1); inhibition of the FnBPB−CDSN interaction by an anti-CDSN antibody (Supporting Figure 2); FnBPB−CDSN interaction is not blocked by a rabbit IgG antibody (Supporting Figure 3); and influence of contact time on the FnBPB−CDSN interaction (Supporting Figure 4) (PDF)

AUTHOR INFORMATION

Corresponding Authors

Joan A. Geoghegan − *Department of Microbiology, Moyne Institute of Preventive Medicine, School of Genetics and Microbiology, Trinity College Dublin, Dublin 2, Ireland; Institute of Microbiology and Infection, University of Birmingham, Birmingham B15 2TT, U.K.*; Email: j.geoghegan@bham.ac.uk

Yves F. Dufrêne − *Louvain Institute of Biomolecular Science and Technology, UCLouvain, B-1348 Louvain-la-Neuve, Belgium*; orcid.org/0000-0002-7289-4248; Email: yves.dufrene@uclouvain.be

Authors

Telmo O. Paiva − *Louvain Institute of Biomolecular Science and Technology, UCLouvain, B-1348 Louvain-la-Neuve, Belgium*

https://doi.org/10.1021/acsnanoscienceau.2c00036
ACS Nanosci. Au XXXX, XXX, XXX−XXX

Albertus Viljoen − *Louvain Institute of Biomolecular Science and Technology, UCLouvain, B-1348 Louvain-la-Neuve, Belgium*

Thaina M. da Costa − *Department of Microbiology, Moyne Institute of Preventive Medicine, School of Genetics and Microbiology, Trinity College Dublin, Dublin 2, Ireland*

Complete contact information is available at: https://pubs.acs.org/10.1021/acsnanoscienceau.2c00036

Author Contributions

[‖]T.O.P. and A.V. contributed equally. T.O.P, A.V., J.A.G., and Y.F.D. contributed to the design of experiments, data interpretation, and writing of the paper. T.M.D.C. generated biological tools. T.O.P. and A.V. performed the experiments and collected the data.

Notes

The authors declare no competing financial interest.

■ ACKNOWLEDGMENTS

Work at the Université Catholique de Louvain was supported by the European Research Council (ERC) under the European Union's Horizon 2020 research and innovation program (grant agreement no. 693630), the Excellence of Science-EOS programme (Grant #30550343), and the National Fund for Scientific Research (FNRS). Y.F.D. is Research Director at the FNRS. The research conducted at Trinity College Dublin was funded by the Irish Research Council under grant number GOIPD/2018/709′.

■ REFERENCES

(1) Cassini, A.; Högberg, L. D.; Plachouras, D.; Quattrocchi, A.; Hoxha, A.; Simonsen, G. S.; Colomb-Cotinat, M.; Kretzschmar, M. E.; Devleesschauwer, B.; Cecchini, M.; Ouakrim, D. A.; Oliveira, T. C.; Struelens, M. J.; Suetens, C.; Monnet, D. L.; Strauss, R.; Mertens, K.; Struyf, T.; Catry, B.; Latour, K.; Ivanov, I. N.; Dobreva, E. G.; Andraševic, A. T.; Soprek, S.; Budimir, A.; Paphitou, N.; Žemlicková, H.; Olsen, S. S.; Sönksen, U. W.; Märtin, P.; Ivanova, M.; Lyytikäinen, O.; Jalava, J.; Coignard, B.; Eckmanns, T.; Sin, M. A.; Haller, S.; Daikos, G. L.; Gikas, A.; Tsiodras, S.; Kontopidou, F.; Tóth, Á.; Hajdu, Á.; Guólaugsson, Ó.; Kristinsson, K. G.; Murchan, S.; Burns, K.; Pezzotti, P.; Gagliotti, C.; Dumpis, U.; Liuimiene, A.; Perrin, M.; Borg, M. A.; Greeff, S. C. de.; Monen, J. C.; Koek, M. B.; Elstrøm, P.; Zabicka, D.; Deptula, A.; Hryniewicz, W.; Caniça, M.; Nogueira, P. J.; Fernandes, P. A.; Manageiro, V.; Popescu, G. A.; Serban, R. I.; Schréterová, E.; Litvová, S.; Štefkovicová, M.; Kolman, J.; Klavs, I.; Korošec, A.; Aracil, B.; Asensio, A.; Pérez-Vázquez, M.; Billström, H.; Larsson, S.; Reilly, J. S.; Johnson, A.; Hopkins, S. Attributable Deaths and Disability-Adjusted Life-Years Caused by Infections with Antibiotic-Resistant Bacteria in the EU and the European Economic Area in 2015: A Population-Level Modelling Analysis. *Lancet Infect. Dis.* **2019**, *19*, 56−66.

(2) Tong, S. Y. C.; Davis, J. S.; Eichenberger, E.; Holland, T. L.; Fowler, V. G. *Staphylococcus aureus* Infections: Epidemiology, Pathophysiology, Clinical Manifestations, and Management. *Clin. Microbiol. Rev.* **2015**, *28*, 603−661.

(3) Bieber, T. Atopic Dermatitis. *N. Engl. J. Med.* **2008**, *358*, 1483−1494.

(4) Wertheim, H. F. L.; Vos, M. C.; Ott, A.; van Belkum, A.; Voss, A.; Kluytmans, J. A. J. W.; van Keulen, P. H. J.; Vandenbroucke-Grauls, C. M. J. E.; Meester, M. H. M.; Verbrugh, H. A. Risk and Outcome of Nosocomial *Staphylococcus aureus* Bacteraemia in Nasal Carriers versus Non-Carriers. *Lancet* **2004**, *364*, 703−705.

(5) Totté, J. E. E.; van der Feltz, W. T.; Hennekam, M.; van Belkum, A.; van Zuuren, E. J.; Pasmans, S. G. M. A. Prevalence and Odds of *Staphylococcus aureus* Carriage in Atopic Dermatitis: A Systematic Review and Meta-Analysis. *Br. J. Dermatol.* **2016**, *175*, 687−695.

(6) Kong, H. H.; Oh, J.; Deming, C.; Conlan, S.; Grice, E. A.; Beatson, M. A.; Nomicos, E.; Polley, E. C.; Komarow, H. D.; Murray, P. R.; Turner, M. L.; Segre, J. A.; NISC Comparative Sequence Program. Temporal Shifts in the Skin Microbiome Associated with Disease Flares and Treatment in Children with Atopic Dermatitis. *Genome Res.* **2012**, *22*, 850−859.

(7) Tauber, M.; Balica, S.; Hsu, C.-Y.; Jean-Decoster, C.; Lauze, C.; Redoules, D.; Viodé, C.; Schmitt, A.-M.; Serre, G.; Simon, M.; Paul, C. F. *Staphylococcus aureus* Density on Lesional and Nonlesional Skin Is Strongly Associated with Disease Severity in Atopic Dermatitis. *J. Allergy Clin. Immunol.* **2016**, *137*, 1272−1274.e3.

(8) Cho, S. H.; Strickland, I.; Boguniewicz, M.; Leung, D. Y. Fibronectin and Fibrinogen Contribute to the Enhanced Binding of *Staphylococcus aureus* to Atopic Skin. *J. Allergy Clin. Immunol.* **2001**, *108*, 269−274.

(9) Fleury, O. M.; McAleer, M. A.; Feuillie, C.; Formosa-Dague, C.; Sansevere, E.; Bennett, D. E.; Towell, A. M.; McLean, W. H. I.; Kezic, S.; Robinson, D. A.; Fallon, P. G.; Foster, T. J.; Dufrêne, Y. F.; Irvine, A. D.; Geoghegan, J. A. Clumping Factor B Promotes Adherence of *Staphylococcus aureus* to Corneocytes in Atopic Dermatitis. *Infect. Immun.* **2017**, *85*, No. e00994-16.

(10) Feuillie, C.; Vitry, P.; McAleer, M. A.; Kezic, S.; Irvine, A. D.; Geoghegan, J. A.; Dufrêne, Y. F. Adhesion of *Staphylococcus aureus* to Corneocytes from Atopic Dermatitis Patients Is Controlled by Natural Moisturizing Factor Levels. *mBio* **2018**, *9*, No. e01184-18.

(11) Towell, A. M.; Feuillie, C.; Vitry, P.; Da Costa, T. M.; Mathelié-Guinlet, M.; Kezic, S.; Fleury, O. M.; McAleer, M. A.; Dufrêne, Y. F.; Irvine, A. D.; Geoghegan, J. A. *Staphylococcus aureus* Binds to the N-Terminal Region of Corneodesmosin to Adhere to the Stratum Corneum in Atopic Dermatitis. *Proc. Natl. Acad. Sci. U.S.A.* **2021**, *118*, No. e2014444118.

(12) Jonca, N.; Guerrin, M.; Hadjiolova, K.; Caubet, C.; Gallinaro, H.; Simon, M.; Serre, G. Corneodesmosin, a Component of Epidermal Corneocyte Desmosomes, Displays Homophilic Adhesive Properties. *J. Biol. Chem.* **2002**, *277*, 5024−5029.

(13) Riethmuller, C.; McAleer, M. A.; Koppes, S. A.; Abdayem, R.; Franz, J.; Haftek, M.; Campbell, L. E.; MacCallum, S. F.; McLean, W. H. I.; Irvine, A. D.; Kezic, S. Filaggrin Breakdown Products Determine Corneocyte Conformation in Patients with Atopic Dermatitis. *J. Allergy Clin. Immunol.* **2015**, *136*, 1573−1580.e2.

(14) Steinert, P. M.; Mack, J. W.; Korge, B. P.; Gan, S. Q.; Haynes, S. R.; Steven, A. C. Glycine Loops in Proteins: Their Occurrence in Certain Intermediate Filament Chains, Loricrins and Single-Stranded RNA Binding Proteins. *Int. J. Biol. Macromol.* **1991**, *13*, 130−139.

(15) Caubet, C.; Jonca, N.; Lopez, F.; Estève, J.-P.; Simon, M.; Serre, G. Homo-Oligomerization of Human Corneodesmosin Is Mediated by Its N-Terminal Glycine Loop Domain. *J. Invest. Dermatol.* **2004**, *122*, 747−754.

(16) Burke, F. M.; McCormack, N.; Rindi, S.; Speziale, P.; Foster, T. J. Fibronectin-Binding Protein B Variation in *Staphylococcus aureus*. *BMC Microbiol.* **2010**, *10*, No. 160.

(17) Foster, T. J.; Geoghegan, J. A.; Ganesh, V. K.; Höök, M. Adhesion, Invasion and Evasion: The Many Functions of the Surface Proteins of *Staphylococcus aureus*. *Nat. Rev. Microbiol.* **2014**, *12*, 49−62.

(18) Ponnuraj, K.; Bowden, M. G.; Davis, S.; Gurusiddappa, S.; Moore, D.; Choe, D.; Xu, Y.; Hook, M.; Narayana, S. V. L. A "Dock, Lock, and Latch" Structural Model for a Staphylococcal Adhesin Binding to Fibrinogen. *Cell* **2003**, *115*, 217−228.

(19) Speziale, P.; Pietrocola, G. The Multivalent Role of Fibronectin-Binding Proteins A and B (FnBPA and FnBPB) of *Staphylococcus aureus* in Host Infections. *Front. Microbiol.* **2020**, *11*, No. 2054.

(20) Herman, P.; El-Kirat-Chatel, S.; Beaussart, A.; Geoghegan, J. A.; Foster, T. J.; Dufrêne, Y. F. The Binding Force of the Staphylococcal Adhesin SdrG Is Remarkably Strong. *Mol. Microbiol.* **2014**, *93*, 356−368.

(21) Vitry, P.; Valotteau, C.; Feuillie, C.; Bernard, S.; Alsteens, D.; Geoghegan, J. A.; Dufrêne, Y. F. Force-Induced Strengthening of the Interaction between *Staphylococcus aureus* Clumping Factor B and Loricrin. *mBio* **2017**, *8*, No. e01748-17.
(22) Milles, L. F.; Bernardi, R. C.; Schulten, K.; Gaub, H. E. Molecular Mechanism of Extreme Mechanostability in a Pathogen Adhesin. *Science* **2018**, *359*, 1527−1533.
(23) Herman-Bausier, P.; Dufrêne, Y. F. Force Matters in Hospital-Acquired Infections. *Science* **2018**, *359*, 1464−1465.
(24) Herman-Bausier, P.; Labate, C.; Towell, A. M.; Derclaye, S.; Geoghegan, J. A.; Dufrêne, Y. F. *Staphylococcus aureus* Clumping Factor A Is a Force-Sensitive Molecular Switch That Activates Bacterial Adhesion. *Proc. Natl. Acad. Sci. U.S.A.* **2018**, *115*, 5564−5569.
(25) Pietrocola, G.; Nobile, G.; Gianotti, V.; Zapotoczna, M.; Foster, T. J.; Geoghegan, J. A.; Speziale, P. Molecular Interactions of Human Plasminogen with Fibronectin-Binding Protein B (FnBPB), a Fibrinogen/Fibronectin-Binding Protein from *Staphylococcus aureus*. *J. Biol. Chem.* **2016**, *291*, 18148−18162.
(26) Keane, F. M.; Loughman, A.; Valtulina, V.; Brennan, M.; Speziale, P.; Foster, T. J. Fibrinogen and Elastin Bind to the Same Region within the A Domain of Fibronectin Binding Protein A, an MSCRAMM of *Staphylococcus aureus*. *Mol. Microbiol.* **2007**, *63*, 711−723.
(27) Foster, T. J. The Remarkably Multifunctional Fibronectin Binding Proteins of *Staphylococcus aureus*. *Eur. J. Clin. Microbiol. Infect. Dis.* **2016**, *35*, 1923−1931.
(28) Herman, P.; Pietrocola, G.; Foster, T. J.; Speziale, P.; Dufrêne, Y. Fibrinogen Activates the Capture of Human Plasminogen by Staphylococcal Fibronectin-Binding Proteins. *mBio* **2017**, *8*, No. e01067.
(29) Hinterdorfer, P.; Dufrêne, Y. F. Detection and Localization of Single Molecular Recognition Events Using Atomic Force Microscopy. *Nat. Methods* **2006**, *3*, 347−355.
(30) Xiao, J.; Dufrêne, Y. F. Optical and Force Nanoscopy in Microbiology. *Nat. Microbiol.* **2016**, *1*, No. 16186.
(31) Dufrêne, Y. F. Towards Nanomicrobiology Using Atomic Force Microscopy. *Nat. Rev. Microbiol* **2008**, *6*, 674−680.
(32) Viljoen, A.; Mathelié-Guinlet, M.; Ray, A.; Strohmeyer, N.; Oh, Y. J.; Hinterdorfer, P.; Müller, D. J.; Alsteens, D.; Dufrêne, Y. F. Force Spectroscopy of Single Cells Using Atomic Force Microscopy. *Nat. Rev. Methods Primers* **2021**, *1*, No. 63.
(33) Changeux, J.-P.; Christopoulos, A. Allosteric Modulation as a Unifying Mechanism for Receptor Function and Regulation. *Cell* **2016**, *166*, 1084−1102.
(34) Zhu, R.; Sandtner, W.; Ahiable, J. E. A.; Newman, A. H.; Freissmuth, M.; Sitte, H. H.; Hinterdorfer, P. Allosterically Linked Binding Sites in Serotonin Transporter Revealed by Single Molecule Force Spectroscopy. *Front. Mol. Biosci.* **2020**, *7*, No. 99.
(35) Burke, F. M.; Di Poto, A.; Speziale, P.; Foster, T. J. The A Domain of Fibronectin-Binding Protein B of *Staphylococcus aureus* Contains a Novel Fibronectin Binding Site. *FEBS J.* **2011**, *278*, 2359−2371.
(36) Ganesh, V. K.; Rivera, J. J.; Smeds, E.; Ko, Y.-P.; Bowden, M. G.; Wann, E. R.; Gurusiddappa, S.; Fitzgerald, J. R.; Höök, M. A Structural Model of the *Staphylococcus Aureus* ClfA−Fibrinogen Interaction Opens New Avenues for the Design of Anti-Staphylococcal Therapeutics. *PLoS Pathog.* **2008**, *4*, No. e1000226.
(37) Stemberk, V.; Jones, R. P. O.; Moroz, O.; Atkin, K. E.; Edwards, A. M.; Turkenburg, J. P.; Leech, A. P.; Massey, R. C.; Potts, J. R. Evidence for Steric Regulation of Fibrinogen Binding to *Staphylococcus aureus* Fibronectin-Binding Protein A (FnBPA). *J. Biol. Chem.* **2014**, *289*, 12842−12851.
(38) Merkel, R.; Nassoy, P.; Leung, A.; Ritchie, K.; Evans, E. Energy Landscapes of Receptor-Ligand Bonds Explored with Dynamic Force Spectroscopy. *Nature* **1999**, *397*, 50−53.
(39) Dufrêne, Y. F.; Viljoen, A.; Mignolet, J.; Mathelié-Guinlet, M. AFM in Cellular and Molecular Microbiology. *Cell Microbiol.* **2021**, *23*, No. e13324.
(40) Mathelié-Guinlet, M.; Viela, F.; Alsteens, D.; Dufrêne, Y. F. Stress-Induced Catch-Bonds to Enhance Bacterial Adhesion. *Trends Microbiol.* **2021**, *29*, 286−288.
(41) Mathelié-Guinlet, M.; Viela, F.; Pietrocola, G.; Speziale, P.; Alsteens, D.; Dufrêne, Y. F. Force-Clamp Spectroscopy Identifies a Catch Bond Mechanism in a Gram-Positive Pathogen. *Nat. Commun.* **2020**, *11*, No. 5431.
(42) Zhang, Y.; Wu, M.; Hang, T.; Wang, C.; Yang, Y.; Pan, W.; Zang, J.; Zhang, M.; Zhang, X. *Staphylococcus aureus* SdrE Captures Complement Factor H's C-Terminus via a Novel 'close, Dock, Lock and Latch' Mechanism for Complement Evasion. *Biochem. J.* **2017**, *474*, 1619−1631.
(43) Zong, Y.; Xu, Y.; Liang, X.; Keene, D. R.; Höök, A.; Gurusiddappa, S.; Höök, M.; Narayana, S. V. L. A 'Collagen Hug' Model for *Staphylococcus aureus* CNA Binding to Collagen. *EMBO J.* **2005**, *24*, 4224−4236.
(44) Grandbois, M.; Beyer, M.; Rief, M.; Clausen-Schaumann, H.; Gaub, H. How Strong Is a Covalent Bond? *Science* **1999**, *283*, 1727−1730.
(45) Fritz, J.; Katopodis, A. G.; Kolbinger, F.; Anselmetti, D. Force-Mediated Kinetics of Single P-Selectin/Ligand Complexes Observed by Atomic Force Microscopy. *Proc. Natl. Acad. Sci. U.S.A.* **1998**, *95*, 12283−12288.
(46) Baumgartner, W.; Hinterdorfer, P.; Ness, W.; Raab, A.; Vestweber, D.; Schindler, H.; Drenckhahn, D. Cadherin Interaction Probed by Atomic Force Microscopy. *Proc. Natl. Acad. Sci. U.S.A.* **2000**, *97*, 4005−4010.
(47) Dupres, V.; Menozzi, F. D.; Locht, C.; Clare, B. H.; Abbott, N. L.; Cuenot, S.; Bompard, C.; Raze, D.; Dufrêne, Y. F. Nanoscale Mapping and Functional Analysis of Individual Adhesins on Living Bacteria. *Nat. Methods* **2005**, *2*, 515−520.
(48) Müller, D. J.; Helenius, J.; Alsteens, D.; Dufrêne, Y. F. Force Probing Surfaces of Living Cells to Molecular Resolution. *Nat. Chem. Biol.* **2009**, *5*, 383−390.
(49) Milles, L. F.; Gaub, H. E. Extreme Mechanical Stability in Protein Complexes. *Curr. Opin. Struct. Biol.* **2020**, *60*, 124−130.
(50) Bernardi, R. C.; Durner, E.; Schoeler, C.; Malinowska, K. H.; Carvalho, B. G.; Bayer, E. A.; Luthey-Schulten, Z.; Gaub, H. E.; Nash, M. A. Mechanisms of Nanonewton Mechanostability in a Protein Complex Revealed by Molecular Dynamics Simulations and Single-Molecule Force Spectroscopy. *J. Am. Chem. Soc.* **2019**, *141*, 14752−14763.
(51) Liu, Z.; Liu, H.; Vera, A. M.; Bernardi, R. C.; Tinnefeld, P.; Nash, M. A. High Force Catch Bond Mechanism of Bacterial Adhesion in the Human Gut. *Nat. Commun.* **2020**, *11*, No. 4321.
(52) Schoeler, C.; Malinowska, K. H.; Bernardi, R. C.; Milles, L. F.; Jobst, M. A.; Durner, E.; Ott, W.; Fried, D. B.; Bayer, E. A.; Schulten, K.; Gaub, H. E.; Nash, M. A. Ultrastable Cellulosome-Adhesion Complex Tightens under Load. *Nat. Commun.* **2014**, *5*, No. 5635.
(53) Otto, M. Physical Stress and Bacterial Colonization. *FEMS Microbiol. Rev.* **2014**, *38*, 1250−1270.
(54) Sedlak, S. M.; Schendel, L. C.; Melo, M. C. R.; Pippig, D. A.; Luthey-Schulten, Z.; Gaub, H. E.; Bernardi, R. C. Direction Matters: Monovalent Streptavidin/Biotin Complex under Load. *Nano Lett.* **2019**, *19*, 3415−3421.
(55) Sokurenko, E. V.; Vogel, V.; Thomas, W. E. Catch-Bond Mechanism of Force-Enhanced Adhesion: Counterintuitive, Elusive, but··· Widespread? *Cell Host Microbe* **2008**, *4*, 314−323.
(56) O'Neill, E.; Pozzi, C.; Houston, P.; Humphreys, H.; Robinson, D. A.; Loughman, A.; Foster, T. J.; O'Gara, J. P. A Novel *Staphylococcus aureus* Biofilm Phenotype Mediated by the Fibronectin-Binding Proteins, FnBPA and FnBPB. *J. Bacteriol.* **2008**, *190*, 3835−3850.

https://doi.org/10.1021/acsnanoscienceau.2c00036
ACS Nanosci. Au XXXX, XXX, XXX−XXX